Spectrum of Engineering Sciences
ISSN (e) 3007-3138 (p) 3007-312X Volume 3, Issue 4, 2025

IDENTIFICATION OF SUBSURFACE SULFIDE ORE DEPOSITS USING GROUND MAGNETIC EXPLORATION TECHNIQUE: A CASE STUDY FROM DROSH-KALDAM GOL, CHITRAL, NORTHERN PAKISTAN

Azeem Khan[*1], Khaista Rehman[2], Asghar Ali[3]

*[*1]PhD Scholar, National Centre of Excellence in Geology, University of Peshawar, Pakistan*
[2]PhD, National Centre of Excellence in Geology, University of Peshawar, Pakistan
[3]PhD, Department of Geology, University of Peshawar, Pakistan

[*1]geoazeemkhan@gmail.com, [2]rehmannceg@uop.edu.pk, [3]asghar.ali@uop.edu.pk

DOI: https://doi.org/10.5281/zenodo.15210370

Keywords
Sulfide minerals, magnetic method, magnetic anomaly, sulfide drilling, porphyry systems

Article History
Received on 07 March 2025
Accepted on 07 April 2025
Published on 14 April 2025

Corresponding Author: * Azeem Khan

Abstract
The ground magnetic data over parts of Gawuch Formation at Drosh-Kaldam Gol, Chitral region has been analyzed both qualitatively and quantitatively with the aim to map subsurface sulfide mineralization, analyze structural lineaments and their influence on mineralization, ascertain the depth of causative source bodies and pinpoint economically viable sulfide drilling prospects in the area. In the study area, the total magnetic intensity values range from a minimum of 48,500 nanoteslas (nT) to a maximum of 56,000 nT, whereas the residual magnetic anomaly levels span from -3000 nT to 4500 nT. The qualitative structural analysis of magnetic data using various visualizations have yielded detailed insights into the subsurface geological features and has successfully pinpointed and delineated numerous anomalous zones (A, B, C, D & E) having the potential for occurrence of sulfide ore minerals and are proposed as a promising drilling targets for sulfide mineral prospection in the area. The quantitative analysis using Peter's half slope and Maximum slope technique indicates that the magnetic anomaly sources in the study area range from near-surface to around 22.37 meters deep, suggesting shallow mineralization targets.
The magnetic data analysis also reveals a shallow and sporadic network of circular to semicircular NE-SW trending magnetic discontinuities/structural lineaments (faults/fractures) which facilitate the process of hydrothermal mobilization and exert a significant impact on the spatial distribution of sulfide mineralization, which is associated with diorite-granodiorite intrusions and displays characteristics typical of porphyry systems. The findings demonstrated that magnetic method is a dependable tool for mapping subsurface structures, which are essential for evaluating the potential of sulfide ore minerals in complex topographic and geological settings.

INTRODUCTION
Hydrothermal deposits are characterized by the presence of ore minerals, primarily sulfides, which tend to precipitate in proximity to faults, fractures, and shear zones (Farhan et al., 2021b). Numerous studies have highlighted the significant role these structural features play in mineralization. It has been shown that faults and fractures are crucial in concentrating various types of deposits, such as

porphyry (Cloos and Sapiie, 2013), epithermal (Chang et al., 2011), and orogenic deposits (Sinclair, 2007; Groves et al., 2018; Gaboury, 2019). Sulfide minerals are highly valuable economically, not only for their primary ore contents such as copper (Cu), lead (Pb), and zinc (Zn), but also for their role as hosts and carriers of additional valuable elements like gold (Au), silver (Ag), arsenic (As), cadmium (Cd), cobalt (Co), bismuth (Bi), mercury (Hg), molybdenum (Mo), antimony (Sb), tin (Sn), nickel (Ni), tellurium (Te), and thallium (Tl) (Norman et al., 2003; Fontboté et al., 2017; Wang et al., 2017). The geophysical properties of sulfide deposits, whether disseminated or massive, differ significantly from those of their host rocks, due to variations in physical and chemical properties (Thomas et al., 2000). For instance, the magnetic properties of certain sulfide minerals, such as pyrrhotite in association with magnetite alters the magnetic profile of the host rock which offer a valuable exploration tool, enabling the detection and delineation of sulfide-rich deposits through magnetic surveys (Ford et al., 2007; Morgan, 2012).

The magnetic method is a widely used passive source geophysical exploration technique that detects subtle changes in the Earth's magnetic field caused by magnetic minerals in rocks, revealing subsurface features like faults, folds, intrusions and magnetic ore deposits (Telford et al,. 2001; Mariita, 2007; Ogagarue and Emudianughe, 2016; Bernard and Renisia, 2014; Shahverdi, 2017). This helps geologists understand an area's geological history, identify potential mineral deposit locations, and focus exploration efforts on promising regions, leading to more efficient and cost-effective resource discovery. Beyond geology, magnetic surveys are also useful in archaeology for finding buried artifacts and in other fields such as hydrology, environmental science, and engineering for assessing subsurface conditions (Stanley et al., 2021; Ogagarue and Emudianughe, 2016; Amigun and Adelusi, 2013; Furness, 2007; Saleem et al., 2002; Weymouth, 1985; Joshua et al., 2017, Mariita, 2007). Thus, magnetic surveys are a versatile and valuable tool providing crucial insights across various scientific domains.

1. Study Area

Pakistan's northern regions exhibit a complex geological framework, stemming from the evolution of the intra-oceanic Kohistan Island Arc and subsequent geological events, rendering them conducive to hosting a diverse array of economic mineral deposits comprising arc and back-arc epithermal precious metal mineralization, as well as arc-related porphyry copper, gold, and molybdenum deposits (Sweatman et al., 1995; PMDC, 2001; Farhan et al., 2021a). The study area, Drosh-Kaldam Gol, located approximately 05 km east of Drosh town in district Chitral, falls within the geographical coordinates of 3938063N to 3940961N latitude and 755613E to 758843E longitude and lies at the north western margin of the Kohistan Island Arc terrane in northern Pakistan (Figs. 1 & 2), is distinguished by the presence of polymetallic sulfide mineralization hosted within the Cretaceous Gawuch Formation’s metavolcanic rocks, which have been intruded by dioritic to granodioritic sills, dykes and quartz veins from the Early Eocene (40–45 Ma) belonging to the Lowari pluton of the Kohistan batholith (Tahirkheli et al., 2005; Tahirkheli et al., 2012; Farhan et al., 2021b). The first systematic exploration work for economic metal potential in Chitral and adjoining regions was initiated by Sarhad Development Authority (SDA) in 1974-78 in collaboration with Austro-minerals by collecting ~2,000 stream sediments samples and covering an area of approximately 80,000 km^2 in northern Pakistan to trace possible lode Cu-Au mineralization in northern Pakistan (Halfpenny and Mazzucchelli, 1999). The samples collected by SDA from the adits, trenches and exposures of sulfide and oxidized zones in Drosh region represented disseminated, massive and vein type mineralization showcasing a diverse array of minerals such as pyrite, chalcopyrite, tetrahedrite, magnetite, malachite and azurite etc. Results of stream sediment surveys suggest that mineralization in the study area is generally controlled by structural features such as faults, fractures and joints and is associated with ferromagnetic minerals like magnetite in Kaldom Gol diorites (Tahirkheli et al., 2012, Ali et al., 2014b). Previous studies in the study area present geochemical and petrographic characteristics of the ore minerals and their host rocks (Tahirkheli et al., 2012; Farhan et al., 2021b), results from fluid inclusion investigation and ages of the ore forming processes (Tahirkheli et al., 1997, Farhan et al., 2023). However, the study area is characterized by a significant lack of geophysical data, particularly with regards to subsurface geology and the extent of sulfide ore deposits, necessitating the application of magnetic geophysical techniques to uncover hidden sulfide ore deposits and delineate underlying structural features; as such resources are frequently located near fault or fracture zones.

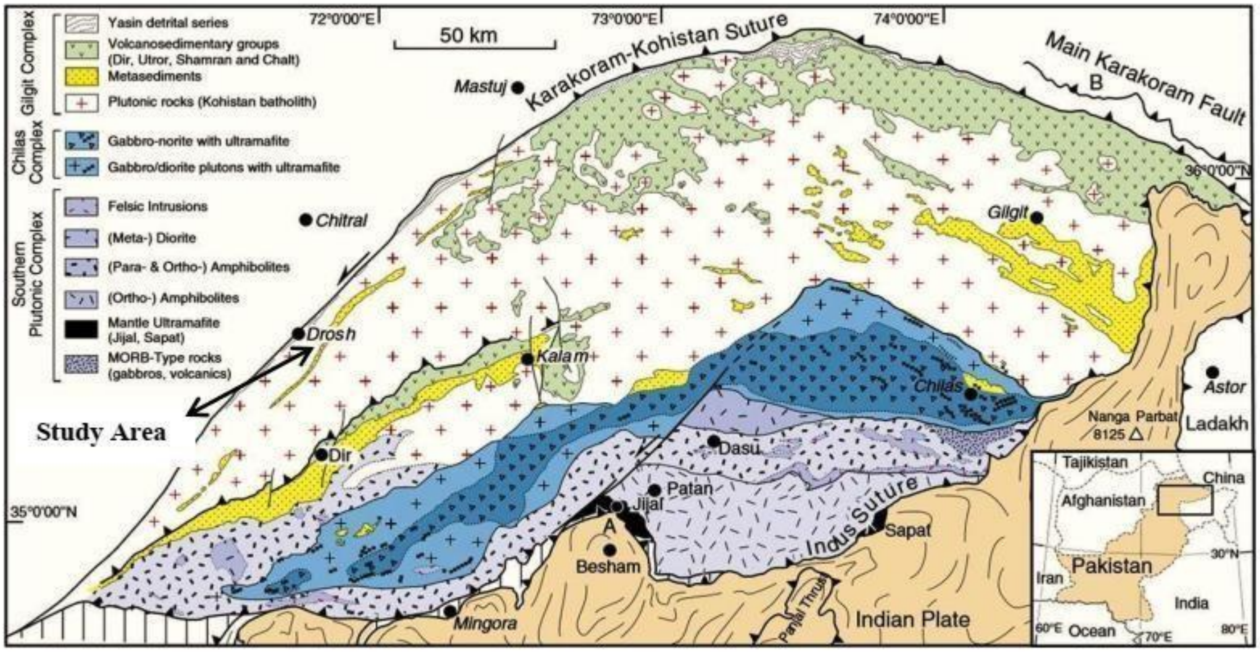

Fig. 1: Geological map of the Kohistan Island Arc, Northern Pakistan, indicating the study area's location (after Ewing & Muntener, 2018).

2. Objectives

The objectives of this study are to thoroughly analyze the subsurface geology/structures of the study area using ground magnetic geophysical techniques, with the goal of assessing the relevance geophysical method in accurately delineating subsurface sulfide ore deposits, evaluating the influence of structural lineaments on mineralization, determining the depth of geophysical anomalies, and identifying promising sites for economically viable drilling.

4. Regional and Local Geological Setting

The geotectonic framework of the northern region of Pakistan consists of three domains, with the Kohistan Island Arc (KIA) sandwiched between the Eurasian plate to the north and the Indian plate to the south (Kazmi and Jan 1997; Faisal et al. 2014; Rehman et al. 2015. The tectonic fabric of the Kohistan Island Arc (KIA) is woven by the intersection of two major faulted suture zones: the Main Mantle Thrust (MMT) or Indus Suture Zone (ISZ) and the Main Karakoram Thrust (MKT) or Shyok Suture Zone (SSZ), which demarcate its northern and southern boundaries, respectively (Pudsey et al., 1985; Coward et al., 1986; Petterson, 2010; Ullah et al., 2022a; Ullah et al., 2022b, Farhan et al., 2023, Fig. 1). A complete cross-sectional exposure of the KIA reveals its partial subduction beneath the Indian terrane and obduction onto the Karakoram/Eurasian terrane, (Khan et al., 1997; Bignold and Treloar, 2003; Bignold et al., 2006). The KIA consists of a varied suite of plutonic and volcanic rocks, ranging from felsic to ultramafic compositions, reflecting its complex geological evolution (Searle et al., 1999; Petterson, 2010).

The study area, located along the northwestern periphery of the Kohistan Island Arc (KIA) in Chitral district, northern Pakistan, features three major tectonic elements, including the Karakoram-Kohistan Suture (or Shyok Suture zone), a volcano-sedimentary sequence, and the Kohistan batholith (Fig. 1). The Shyok Suture zone, a mélange zone, characterized by its varying width, ranging from a narrow, sharp fault to a broad zone up to 4 km wide, marking the continental boundary between the Kohistan and Eurasian landmasses and comprises of ultramafics, marbles, and basalts etc (Pudsey and Maguire, 1986, Khan et al., 1994, Tahirkhel et al., 2005). The study area's volcano-sedimentary sequence displays greater complexity compared to the Yasin-Hunza section of Gilgit Baltistan. According to Pudsey et al. (1985), this sequence can be stratigraphically divided into three distinct units: the Drosh Formation at the top, followed by the Purit Formation, and the Gawuch Formation at the base (Fig. 2).

The Drosh Formation consists of a thick Eocene volcanic sequence of andesitic and dacitic composition, that conformably overlies the Purit Formation, a fluvial-dominated unit comprising reddish shale, conglomerate, sandstone (Pudsey et al., 1985, Farhan et al., 2023). While, the Gawuch Formation, a Mesozoic era sequence of metavolcanites with interbedded metasedimentary units including marbles with marine affinity is distinguished by a consistent NE-SW strike and a steep NW dipping attitude, exhibit an intrusive contact with the Lowari pluton of the Kohistan Batholith to the south and a faulted contact with the Purit Formation (Pudsey et al., 1985, Heuberger, 2004). The Formation's southern or basal section features intensely sheared metabasalts transformed into phyllites, while the upper half consists of alternating layers of metabasalts and carbonate rocks (marbles), intruded by the Kohistan Batholith-derived Eocene diorite and granodiorite sills and dykes, which in turn have been pervasively infiltrated by quartz veins (Tahirkheli et al., 1997, Tahirkheli et al., 2005, Farhan et al., 2023). This setting hosts the Kaldam Gol region's polymetallic sulfide mineralization, characterized by a mineral assemblage comprising pyrite, tetrahedrite, galena, chalcopyrite and magnetite etc which is genetically tied to the dioritic-granodioritic intrusions and quartz veining (Tahirkheli et al., 2012, Farhan et al., 2023), Geochemical analysis of fluid inclusion studies have previously revealed that the quartz veins hosting ore minerals formed from a brine with salinity of 12.28-13.4 wt% NaCl equivalent. While Lead-isotope geochronology constrains the minimum age of ore formation to approximately 42 million years, which postdates the Cretaceous host rock, Gawuch Formation but coincides with the magmatic emplacement of the Lowari pluton (40-45 million years), a dioritic to granodioritic complex (Zeitler, 1985; Tahirkheli et al., 2005, Farhan et al., 2023).

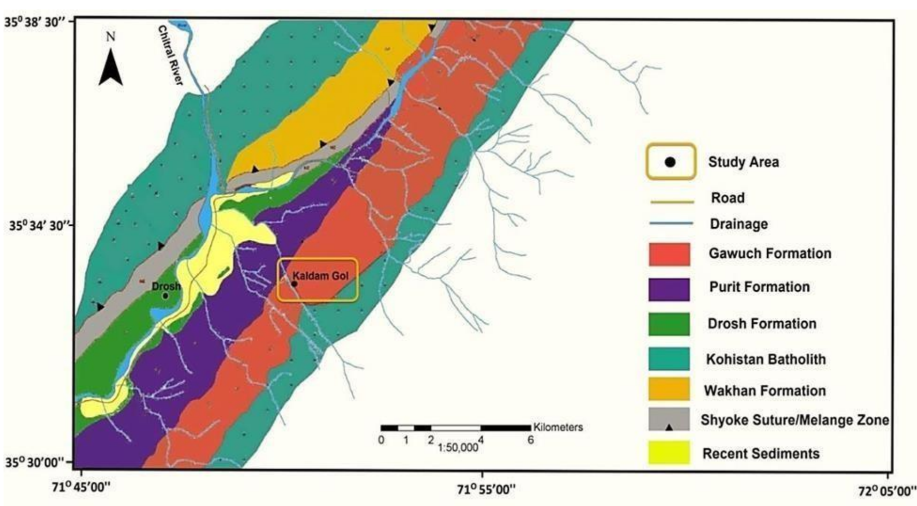

Fig. 2: Geological map of Drosh area, Chitral, Northern Pakistan showing stratigraphic sequences and depicting locality of the study area (after Rasheed et al., 2019).

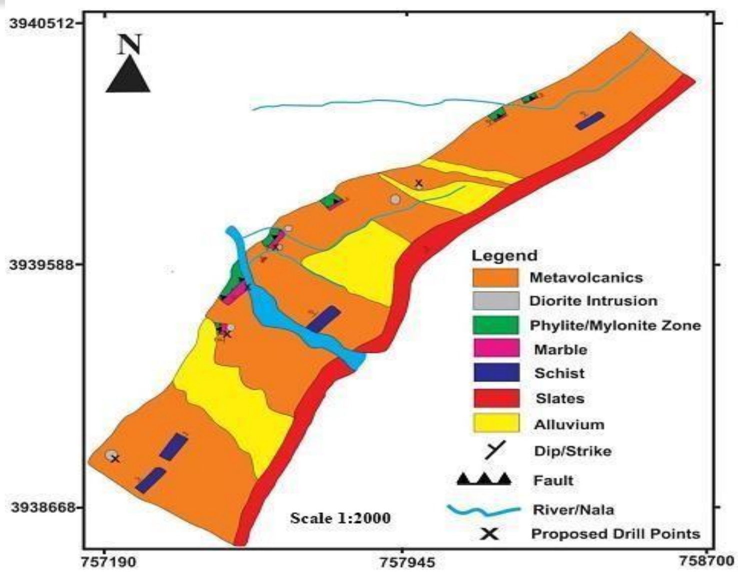

Fig. 3: Geological Map of Gawuch Formation showing litho-stratigraphic units and proposed drill points for sulfide mineral prospection within the study area (Modified after LMPL, 2022).

5. Methods & Materials

This study employed a Geometrics G-858 Cesium Vapor Magnetometer, featuring 0.008 nT sensitivity and 0.2 nT resolution, to measure the total magnetic field intensity across the study area (Figs. 4). Ground magnetic surveys are typically conducted using either a grid pattern or linear profile approach (Ali et al., 2020). However, due to the study area's complex and challenging landscape, a conventional grid-based magnetic survey was not feasible. Instead, geophysical measurements were taken along irregular profiles that followed dry mountainous streams, footpaths, and moderate slope.

Our Geological field investigations in the study area confirm the presence of sulfide mineralization in multiple forms including massive, disseminated and vein type mineralization showcasing primary and supergene sulfide enrichment.

Geophysical profiles were carefully planned based on geological trend analysis and the identification of sulfide, oxidized/altered zones, and mineral showings within the NE-SW trending Gawuch Formation. A detailed magnetic survey was performed, acquiring 506 raw magnetic data points at 10-20 meter station intervals along 30 survey profiles oriented perpendicular or oblique to the Gawuch Formation's NE-SW striking fabric (Fig. 5). In areas with high magnetic gradients, the sampling interval was reduced to 5 meters to ensure detailed coverage. Profile spacing was adaptively varied to accommodate complex topographic and geological features, ensuring optimal data coverage. Due to the use of a single magnetometer, each profile's initial point was re-occupied for repeat measurements, serving as a reference for diurnal corrections. Simultaneously, magnetic data points were precisely geo-located using a handheld Garmin GPS receiver.

Fig. 4: Field photographs showing acquisition of magnetic data using Geometrics G-858 magnetometer across various alteration zones within the Gawuch Formation.

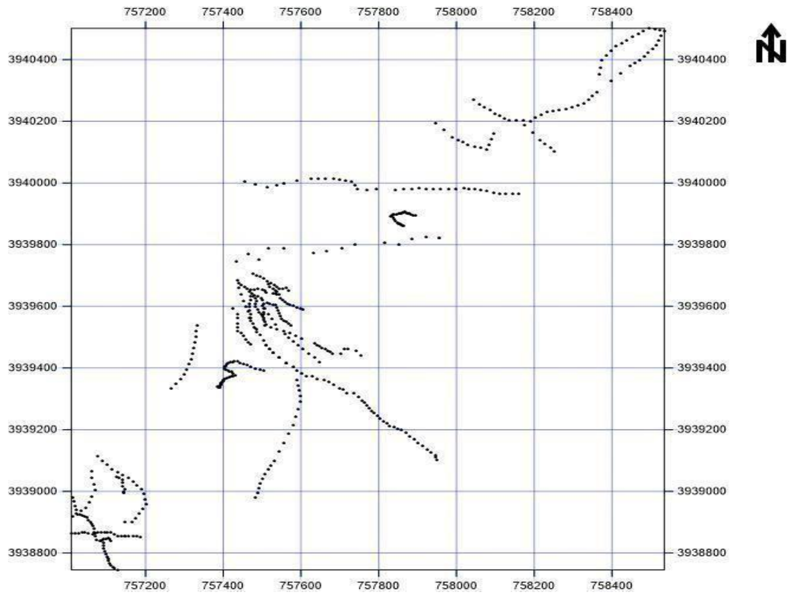

Fig. 5: Illustration showing magnetic data observations/stations recorded in the study area.

6. Magnetic Data Processing

The acquired magnetic data were processed using Golden Surfer software, with diurnal and International Geomagnetic Reference Field (IGRF) corrections applied to remove external magnetic field and geomagnetic effects. The diurnal correction was calculated utilizing the following equations (Ogagarue & Emudianughem, 2016):

$$Dc = \ell \times \Delta T \qquad (1.1)$$

Where,

D_C = Drift or diurnal correction

$\Delta T = T_S - T_{BS}$ = the temporal gap between measurements at the station (S) and the base station (BS) and ℓ is a constant outlined as:

$$\ell = \frac{I_R - I_{In}}{T_R - T_{In}} \qquad (1.2)$$

Where, the notation "In" designates the initial magnetometer reading recorded at the base station, "I_R" signifies the magnetometer reading acquired during the repeat measurement at the base station, and "T_{In}" and "T_R" represent the respective times at which the initial and repeat measurement readings were obtained at the base station

The IGRF model was used to compute the geomagnetic field, incorporating date, elevation, and coordinates from NOAA website (http://www.ngdc.noaa.gov; Amigun and Adelusi, 2013; Eugene et al., 2019). The average IGRF value for the study area was calculated as 51350 nT. The residual magnetic anomaly data were computed by subtracting the average IGRF value from the diurnally corrected magnetic readings at each station (Waswa et al., 2015; Ogagarue & Emudianughem, 2016). These values were subsequently visualized as 2D and 3D maps employing minimum curvature gridding techniques in Surfer Software, thereby highlighting local magnetic signatures.

7. Results

7.1 Qualitative Analysis

The magnetic data collected within the study area is visualized through various representations, including total intensity contour maps, residual magnetic intensity contour maps, and 3D surface distribution maps (Figs. 6a-c) which clearly show parallel to sub parallel, high frequency, short wavelength elliptical or lenticular magnetic ore bodies, characterized by limited extensions occurring adjacently at shallow depths. These visualizations highlights four distinct areas with significant magnetic susceptibility contrast, distinguished by the presence of magnetite-bearing sulfide alteration zones, specifically referred to as zone 01, 02, 03, and 04 (Figs. 6a-b). The magnetic zone division was based on the intensity, shape, and pattern in magnetic signatures alongside mineralization distribution and accessibility approaches in the study area. Within these zones, significant positive and negative magnetic anomalies denoted as A, B, C, D and E have been identified (Fig. 6c).

The total magnetic intensity map depicted in Fig. 6a provides an overview of the absolute strength of the Earth's magnetic field (Telford et al., 1990) across various locations within the study area. In contrast, Fig. 6b, which presents the residual magnetic intensity map, unveils specific localized anomalies or irregularities in Earth's magnetic field. These anomalies become evident after applying corrections for diurnal variations and the International Geomagnetic Reference Field (IGRF) to the total magnetic intensity field data (Otieno, 2012).

In the study area, the total magnetic intensity values range from a minimum of 48,500 nanoteslas (nT) to a maximum of 56,000 nT, While the residual magnetic intensity levels span from -3000 nT to 4500 nT (Figs. 6a-b). The study area exhibits a contrast in magnetic characteristics, with regions of low magnetic intensity indicated by blue to greenish colors and areas of high magnetic intensity depicted by reddish to yellowish hues. These magnetic variations provide insights into the underlying geological features and the degree of subsurface heterogeneity potentially linked to basement structural features like fault or fracture zones in the study area (Ozegin and Alile, 2016).

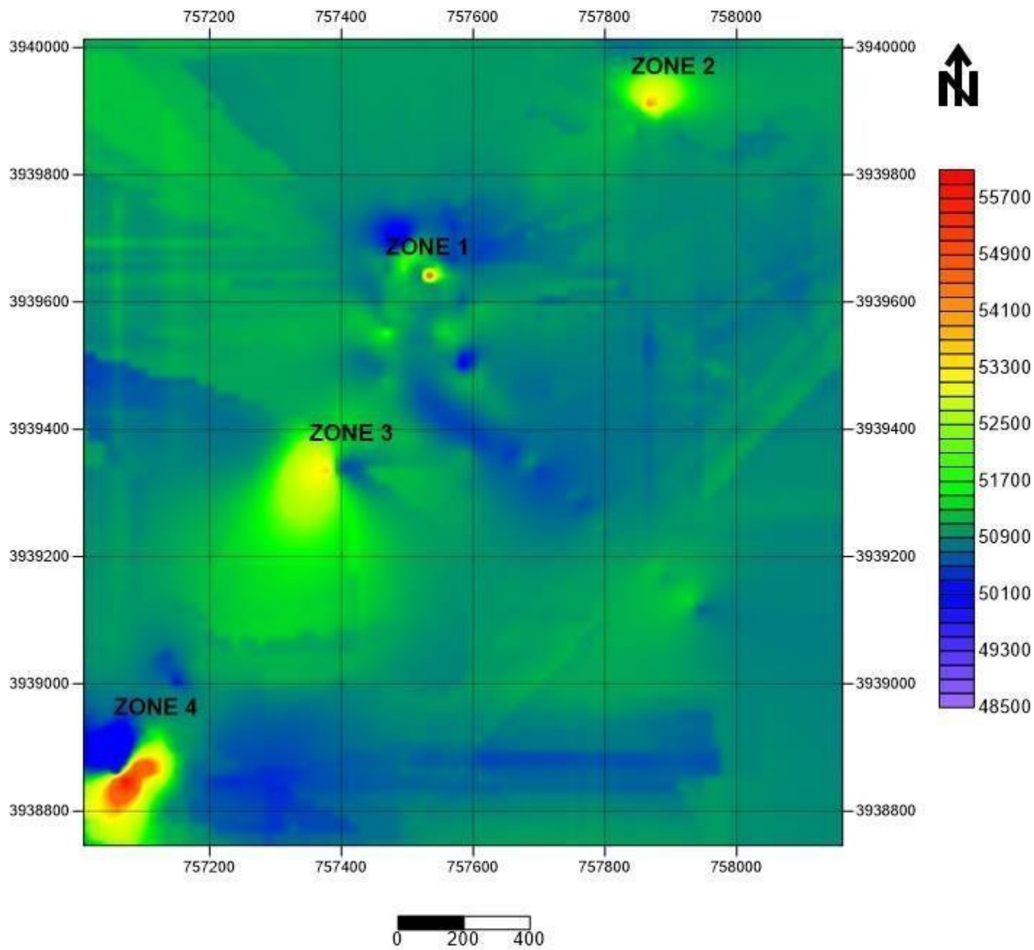
757200
757400
757600
757800
758000
3940000
3939800
3939600
3939400
3939200
3939000
3938800
ZONE 1
ZONE 2
ZONE 3
ZONE 4
N
55700
54900
54100
53300
52500
51700
50900
50100
49300
48500
0
200
400

(a)

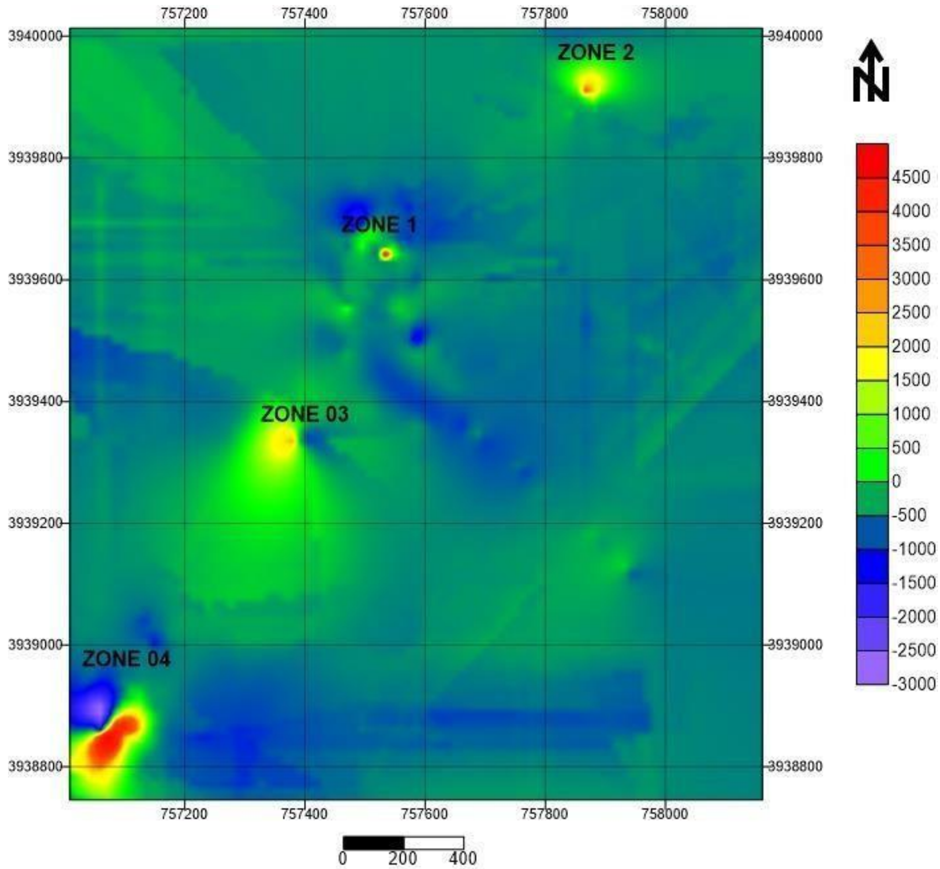

(b)

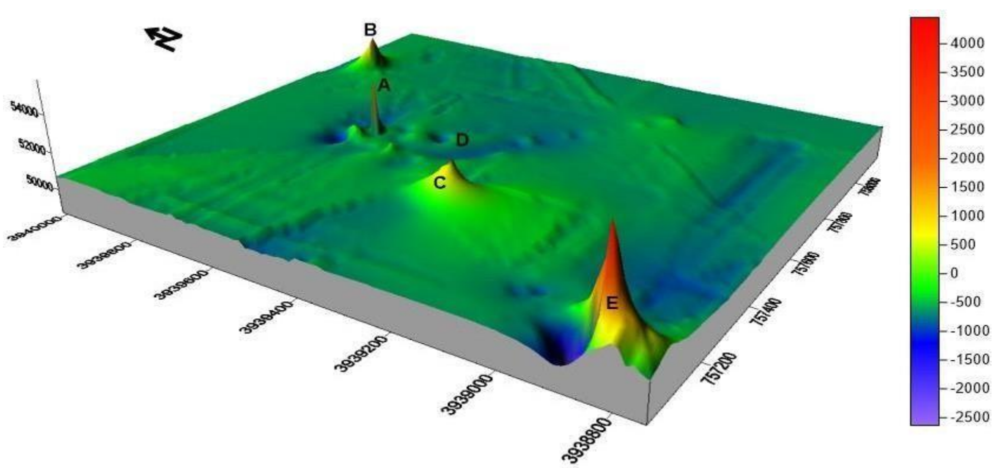

(c)

Fig. 6: Illustrations **(a)** Total magnetic intensity (TMI) ; **(b)** Residual magnetic intensity (RMI) map of the study area showing location of the identified magnetic zones; **(c)** 3D surface distribution map of the study area showing the areas and positions of the identified magnetic anomalies.

i). Zone 01

Zone 01 is located in the low-land region of Kaldam Gol valley and is in close proximity to Kaldam Gol River. Ten magnetic profiles, with lengths ranging from 80 to 400 meters, have been employed to cover this particular zone. In consideration of the topographic conditions and accessibility, a total of 178 magnetic stations were set up along the profiles encircling zone 01. The intervals for these stations were set at either 10 meters or 20 meters, ensuring thorough coverage of the area. After removing the diurnal and regional magnetic field components from the measured magnetic field, a colored Residual Magnetic Intensity (RMI) contour map was generated using Golden Surfer software (Fig. 7a). Within this zone, the RMI levels display a range of high and low magnetic values, varying between 3200 and -1800 nanoteslas (nT), indicating a significant degree of magnetic heterogeneity in the area. The color legend indicates that the reddish to yellow hues represent areas with high magnetic signatures, while the blue to greenish tones denote regions with low magnetic signatures. The residual magnetic image, derived from the difference between Total Magnetic Intensity and IGRF, vividly illustrates the contrasting locations of high and low magnetic intensities, revealing numerous distinct crustal magnetization patterns. Regions exhibiting low magnetic intensity signatures on the magnetic maps/profiles suggest potential discontinuities, faults, or fracture zones whereas, areas characterized by high magnetic intensity indicate the presence of underlying magnetic materials (Feyisa & Gebissa, 2023**).** The magnetic anomaly contours of RMI map of zone 01 are generally elongated in the NE-SW direction which is in accordance with the regional geological strike in the area. In Figures 7a and 7c of zone 01, on the northeastern side, there is a distinct positive magnetic anomaly closure/peak labeled as A. Here, the contour lines form an elliptical closure that is densely packed, indicating a steep gradient or rapid change in magnetic field strength. This suggests a zone characterized by higher magnetic susceptibility, likely indicating the presence of igneous intrusion within the bedrock or an accumulation of ferromagnetic minerals. In addition, there are scattered traces of moderate magnetic signatures virtually all over the area, indicating the presence of blocks or lumps of magnetite within the overburden. The positive anomaly zone of zone 1 spans approximately 30 by 20 meters in surface dimension, with a magnetic anomaly peak measuring 3200 nanoteslas (nT). It exhibits a trend in the NE-SW direction and is encircled by areas characterized by low magnetic intensity patterns. On the other hand relatively low to high amplitude magnetic intensity values between -200 to -1800 nT marked with greenish to blue color forming elliptical to lenticular closures with NE-SW trend are dominated the entire map area (north western, south western, eastern and south eastern) suggesting the presence of shallow subsurface geologic structures and raise the prospect of potential faults or localized fractured zones traversing these area.. While, in the southern region of zone 01, there is a notable elongated low magnetic anomaly feature with contour lines spaced further apart and trending in the NNE-SSW direction. This characteristic suggests the presence of relatively thick overburden or deep-lying source bodies and is interpreted as a potential discontinuity, such as a fault or fracture zone associated with hydrothermally demagnetized fractured rocks in the area.

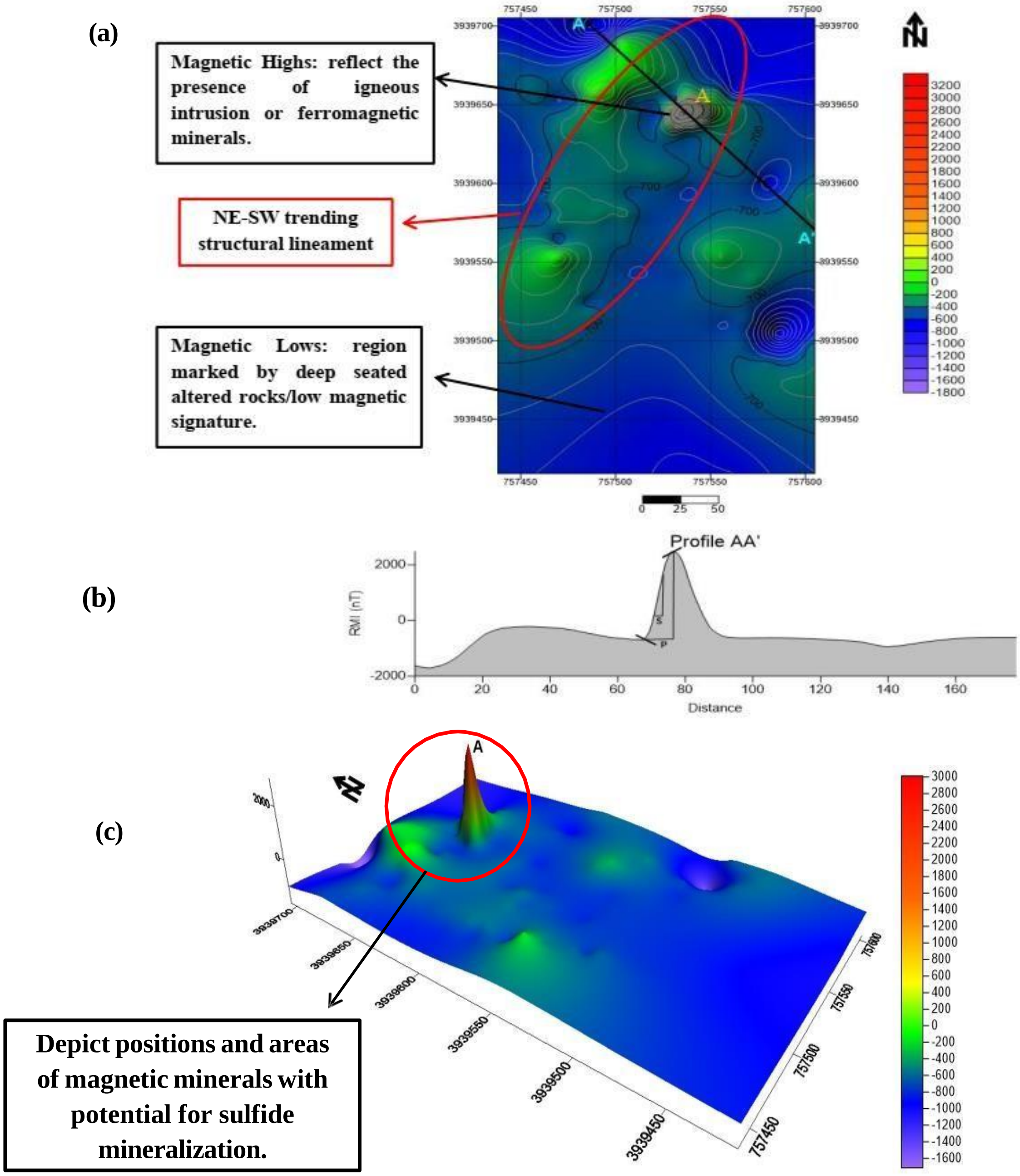

Fig. 07: **(a)** 2D Residual Magnetic Intensity (RMI) contour map of zone 01 showing location of anomaly ‘A’; **(b)** Longitudinal profile section of anomaly ‘A’ using peter half slope (P) and maximum slope (S) methods for depth approximation; **(c)** 3D surface map of zone 01 showing location of anomaly ‘A’.

ii). Zone 02

Zone 02 is situated to the northeast of zone 01, occupying the highland region of the Kaldam Gol valley. This area presented challenges for conducting geophysical profiles due to its steep slopes. Nevertheless, concerted efforts were made to ensure comprehensive coverage of the promising zones within zone 02. The objective was to avoid overlooking any potential mineralized areas in the subsurface, underscoring the dedication to thorough exploration despite challenging terrain. Zone 02 has been surveyed with a total of 08 profiles, with lengths ranging from 80 meters to 700 meters. Along these

profiles, a total of 148 magnetic observations were marked at intervals of either 10 or 20 meters.
The resulting residual magnetic signature reveals significant variations in amplitude, ranging from a minimum value of -1000 nanoteslas (nT) to a maximum of 2800 nT. This variability indicates differing magnetic susceptibilities or variations in the metallic mineral content of the rock types within the surveyed area. A highly magnetic susceptible body/closure/peak trending in the NE-SW direction labeled as anomaly B is prominently visible at the northeastern corner of the RMI and 3D surface maps (Figs. 8a & 8c) which exhibits a magnetic anomaly peak of 2800 nT) and are interpreted as magnetite rich small igneous intrusion which could serves as a prospective site for magnetite associated sulfide mineralization. While, the majority of the map area exhibits a relatively low level of magnetic activity, appearing magnetically quiet or plain. The quiet magnetic zones or subtle magnetic lows that surround isolated high magnetic anomalies may be interpreted as indicative of an alteration zone associated with a potential mineral deposit (Gunn, 1996).

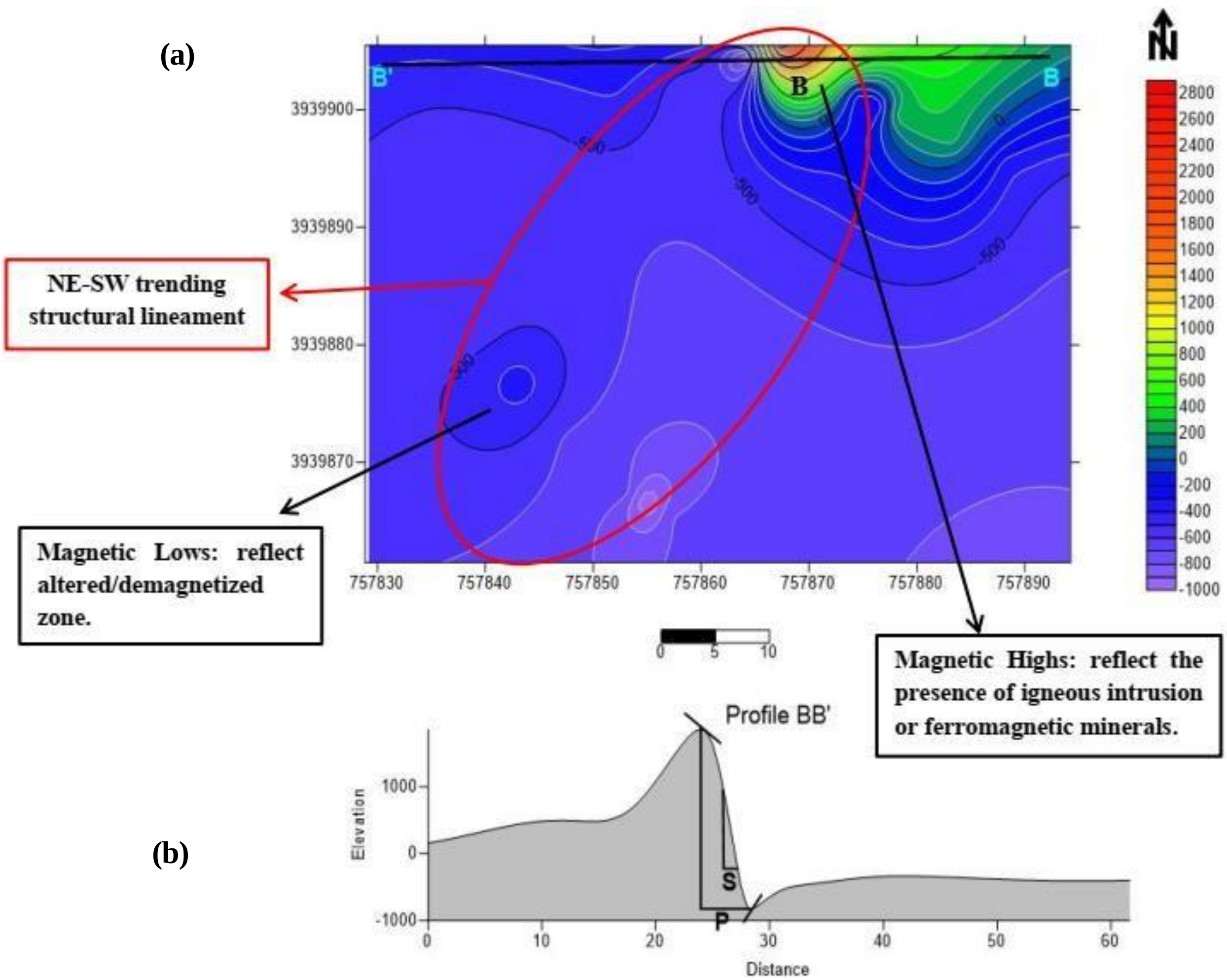

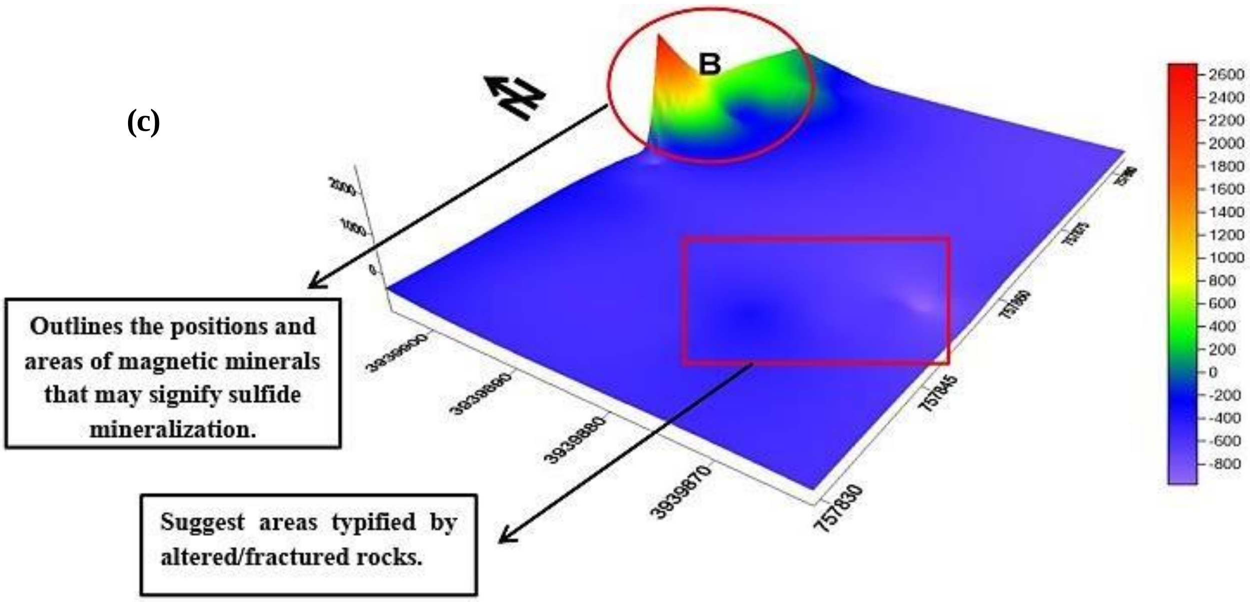

Fig. 08: **(a)** 2D Residual Magnetic Intensity (RMI) contour map of zone 02 showing location of anomaly ‘B’ **(b)** Longitudinal profile section of anomaly ‘B’ using peter half slope (P) and maximum slope (S) methods for depth approximation; **(c)** 3D surface map of zone 02 showing location of anomaly ‘B’.

iii). Zone 03

Zone 03 was surveyed with 04 magnetic profiles ranging from 80 to 400 meters in length, recording a total of 82 magnetic observations at 10 meter and 20 meter intervals along the profiles in this particular zone. The residual magnetic intensity contour map of zone 03 (Fig. 9a) showcases a range of magnetic amplitude characterized by both high and low magnetic intensity values spanning from 1100 nT to -1000 nanoteslas (nT). The magnetic anomaly contours of zone 03 predominantly exhibit a prevailing trend in the NE-SW direction, aligning with the regional geological strike observed in the area. This correspondence highlights the influence of geological factors on the magnetic signature of the region. In the western corner of zone 03 there is an elongated/elliptical contour closure/peak labeled as anomaly C that exhibits a high magnetic signature and is surrounded by regions of low magnetic intensity patterns. It presents a positive anomaly peak of 1100 nT and trends in the NE- SW direction, distinguishing it from the surrounding magnetic characteristics. Based on the analysis of the Residual Magnetic Intensity (RMI) and the 3D surface image (Figs. 9a & 9d) the highly magnetic susceptible body labeled as anomaly C, located at the left corner of zone 03, is interpreted as an igneous intrusion within the bedrock likely containing magnetite associated sulfide mineralization. While towards the northern side of anomaly C, there exists a NE-SW trending lenticular shape, high amplitude (-1000 nT), short wavelength low magnetic intensity feature labeled as anomaly D, depicting areas with near-surface geological structures, possibly fractures or faults, possessing low magnetic contents which could serve as potential hosts for minerals.

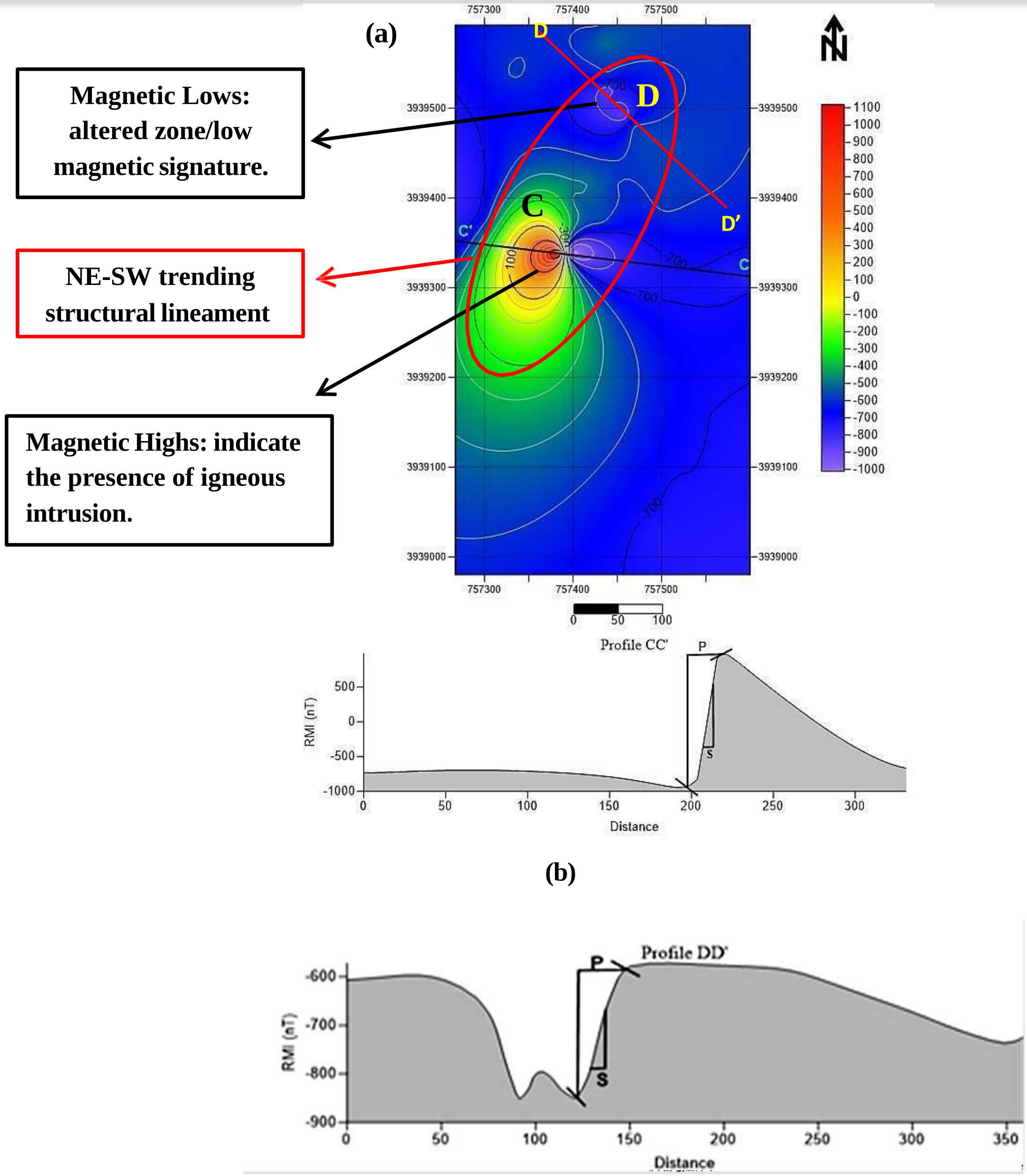
(a)
Magnetic Lows: altered zone/low magnetic signature.
NE-SW trending structural lineament
Magnetic Highs: indicate the presence of igneous intrusion.
D
D'
C
C'
Profile CC'
RMI (nT)
Distance
P
S
(b)
Profile DD'
RMI (nT)
Distance
P
S

(c)

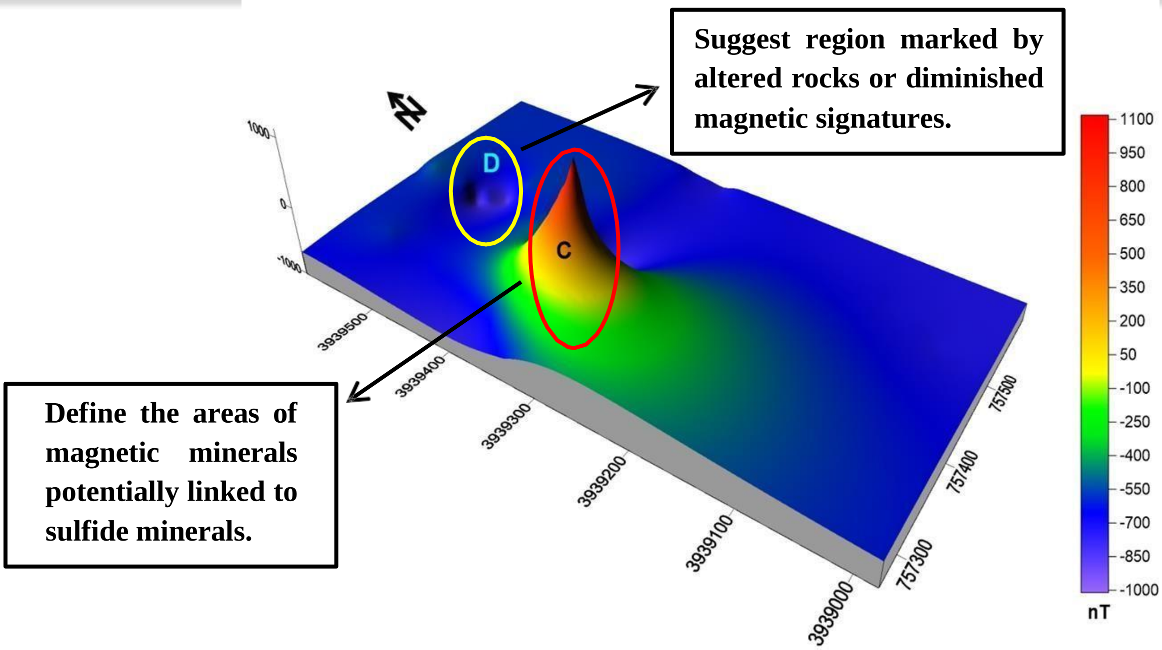

(d)

Fig. 09: **(a)** 2D Residual Magnetic Intensity (RMI) contour map of zone 03 showing location of anomaly 'C' & 'D'; (**b-c)** Longitudinal profile sections of anomaly 'C' & 'D' using peter half slope (P) and maximum slope (S) methods for depth approximation; **(d)** 3D surface map of zone 03 showing location of anomaly 'C' & 'D'.

iv). Zone 04

Zone 04 is situated in the southwestern direction of the study area, within the highland region of the Kaldam Gol valley. Comprehensive coverage of this area was achieved using 08 magnetic profiles, with varying lengths ranging from 80 meters to 200 meters. During the survey, a total of 98 magnetic readings were systematically recorded at intervals of either 10 or 20 meters along the profiles. This approach ensures a thorough examination of the magnetic characteristics specific to zone 04. The Residual Magnetic Intensity (RMI) map of the area (Fig. 10a) illustrates a range of magnetic signatures, with highs reaching a maximum value of 4500 nT and lows dropping to a minimum value of -3000 nT. This variability indicates a magnetic heterogeneity within the area. Notably, the RMI and 3D surface maps reveal the presence of a` dipolar magnetic feature trending in a NE-SW direction, identified as anomaly E (Figs. 10a & 10c). This feature is situated in the southwestern part of zone 04 and exhibits a positive magnetic signature peak of 4500 nT, indicating the likely presence of a magnetite-rich igneous intrusive body in the vicinity. In addition, there are scattered traces of moderate magnetic signatures virtually all over the area, indicating the presence of blocks or lumps of magnetite within the overburden. On the other hand, the northwestern and southeastern parts of the study area exhibit a more prominent low magnetic signature, ranging from -500 nT to -3000 nT. This characteristic suggests potential geological discontinuities, fault, or fracture zone, possibly associated with hydrothermally demagnetized rocks in that region. The NE-SW alignment of the highly magnetic susceptible body/feature (anomaly E), which coincides with the regional geological strike of the area, could potentially serve as the host for magnetite-associated sulfide minerals such as chalcopyrite, pyrhotite, pyrite, galena etc.

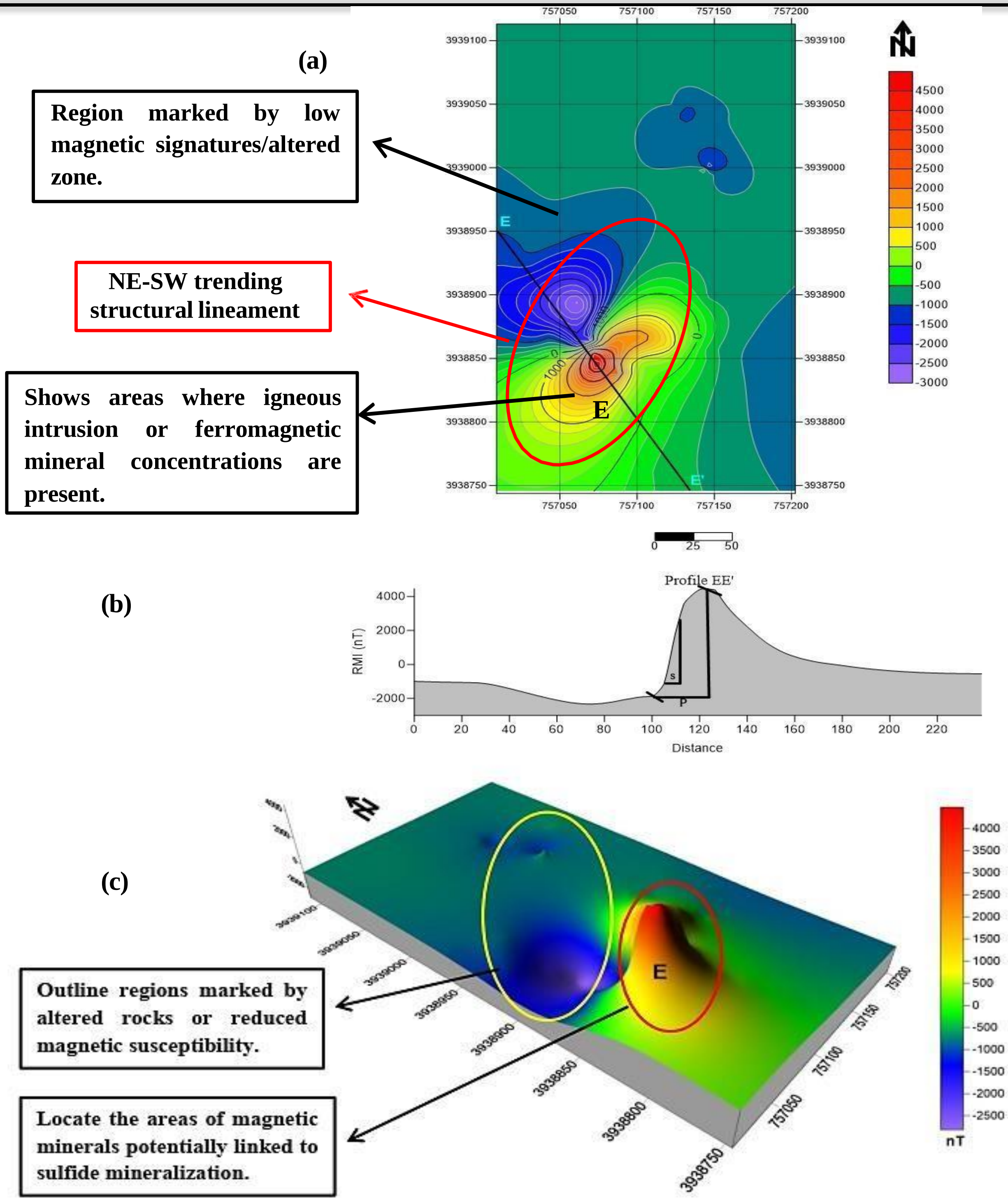

Fig. 10: **(a)** 2D Residual Magnetic Intensity (RMI) contour map of zone 04 showing location of anomaly 'E' **(b)** Longitudinal profile section of anomaly 'E' using peter half slope (P) and maximum slope (S) methods for depth approximation; **(c)** 3D surface map of zone 04 showing location of anomaly 'E'.

7.2 Quantitative Analysis Of Magnetic Data

The depth estimation process represents a quantitative interpretation of geophysical data. The interpretation of geophysical anomalies typically relies on scrutinizing data gathered from specific profiles. The primary aim of this data analysis is to eliminate extraneous signals, ideally retaining only the data that holds geological significance. Numerous methods exist for approximating the depth to the source of anomalies. The key principle is that the depth variation influences the shape of an anomaly. Shallow sources produce narrower and sharper anomalies, while deeper magnetic sources yield broader and flatter anomalies (Abdulbariu et al., 2016, Fig. 11).

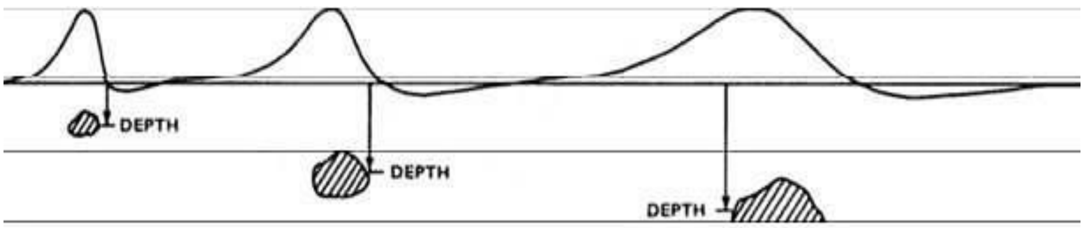

Fig. 11: Impact of depth on the shape and amplitude of anomalies (Abdulbariu et al., 2016).

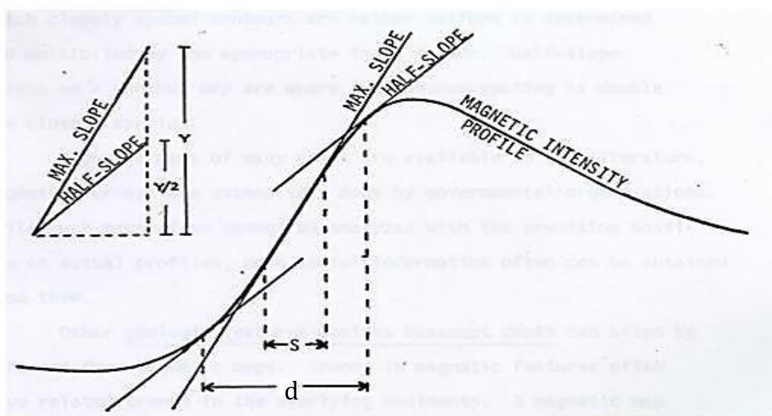

Fig. 12: Magnetic anomaly depth determination: Maximum Slope (S) and Peter's Half-Slope (d) methods (Nettleton, 1971; Telford et al., 1990).

Longitudinal profiles section for the identified magnetic anomalies was produced through Golden Surfer software, visually depicted in Figs. 7b, 8b, 9b-c & 10b. The approximate depth to the top of anomaly sources was determined utilizing graphical approaches, including Peter's half-slope method, and Maximum slope method. The Peter's half-slope and maximum slope techniques leverage the sloping flanks of the profiles, as demonstrated in Fig. 12, for depth estimation (Nettleton, 1971; Telford et al., 1990).

For magnetic depth estimation, either the horizontal extent of the virtually linear segment at the maximum slope (S) or the distance between the two points of tangency, referred to as half slope, (d) is measured. The depth (Z or h) below this segment is then calculated using the following equations (Nwosu and Onuba, 2013; Adegoke et al., 2014).

$Z = KS$; $1.67 \leq K \leq 1.82$ (empirical constant K: 1.82) (1.3)

$d = 1.2 \times h$ (slender body) (1.4)

$d = 1.6 \times h$ (intermediate thickness) (1.5)

$d = 2 \times h$ (very thick body) (1.6)

In Figure 7b for magnetic profile section AA', the depth estimation was derived utilizing both Peter's half-slope and Maximum slope methods, yielding the following results:

Profile	Peter Half Slope Magnetic Curve Depth (m)	Maximum Slope Magnetic Curve Depth (m)	Average Depth
AA'	07.73	07.60	7.68
BB'	02.53	02.54	2.47
CC'	16.40	16.38	16.79
DD'	13.70	13.65	13.61
EE'	22.61	22.02	22.37

Table 01: Summary of depth estimates computed via Peter half slope and maximum slope techniques.

By employing a centimeter ruler, it was established that 8.42 centimeters on the "distance" axis in Figure 7b corresponds to a distance of 160 meters.

$$8.42 \text{ cm} = 160 \text{ m}$$
$$01 \text{ cm} = x$$
$$\Rightarrow x = 01 \text{ cm} = 19 \text{ m}$$

The horizontal distance between the two tangents is $d = 0.624$ cm.

Hence,

$$d = 0.624 \times 19 = 11.85 \text{ m}$$

For a slender body, $d = 1.2$ x h:

$$h \text{ (depth)} = 11.85/1.2 = 9.87 \text{ m}$$

For body of intermediate thickness, $d = 1.6$ x h:

$$, h \text{ (depth)} = 11.85/1.6 = 7.40 \text{ m}$$

For very thick body, $d = 2$ x h:

$$h \text{ (depth)} = 11.85/2.0 = 5.92 \text{ m}$$

Average Depth = 7.73 m

Likewise, employing the maximum slope method for profile AA':

$$S = 0.222 \text{ cm}$$
$$\Rightarrow 0.22 \text{ x } 19 = 4.18$$

Consequently,

$$Z = K_1 S (\text{empirical constant } K_1 = 1.82)$$

$$\text{Depth, } Z = 1.82 \text{ x } 4.18 = 7.60 \text{ m.}$$

Additionally, Table 01 provides a summary of the estimated depths obtained from the longitudinal profile sections of the identified magnetically anomalous zones.

8. Discussions

The ground magnetic data acquired over parts of the Gawuch Formation at Drosh-Kaldam Gol, Chitral region have been interpreted both qualitatively and quantitatively. Qualitatively, the magnetic data is visualized through various representations, including total intensity contour maps, residual magnetic intensity contour maps and 3D surface distribution maps. These visualizations highlights four distinct zones with notable magnetic contrasts, distinguished by the presence of magnetite bearing sulfide alteration zones, specifically referred to as zone 01, 02, 03, and 04 (Figs. 6a-b). Within these zones significant positive and negative magnetic anomaly closures denoted as A, B, C, D and E have been identified (Figs. 7-10). The high magnetic anomalies A, B, C & E identified in zone 01, 02, 03 and 04 of the study area predominantly trending in the NE-SW direction and exhibits elliptical/elongated contour closures with positive magnetic signature peaks of 3200 nT, 2800 nT, 1100 nT and 4500 nT whereas anomaly D in zone 03 with NE-SW trend presents a negative anomaly peak of 1000 nT. The elongated or lenticular nature of magnetic anomaly contours and profile sections analysis indicates that sulfide mineralization in the study area occurs as discontinuous; steeply dipping veins/lenses, or patches. Structural disruption from localized faults and fractures has fragmented these bodies, creating a characteristic pinch-and-swell pattern across the deposit.

Regions exhibiting low magnetic intensity signatures on the magnetic profiles/maps are attributed to faults or a highly fractured terrain in the area where the influence of hydrothermal fluid flow during weathering or oxidation processes leads to the potential depletion and alteration of magnetite to minerals like hematite or other non-magnetic minerals with lower magnetic responses compared to the surrounding rocks (Reeves 2005; Tawey et al. 2020), whereas areas characterized by high magnetic intensity may point to the presence of potentially small, shallow mineralized intrusions/plugs of intermediate to basic composition within the bedrock which could potentially serve as prospective sites for magnetite-associated sulfide mineral mineralization in the study are. The high magnetic anomaly clusters labeled as A in zone 1 has an approximate surface extent of 30 by 20 meters, anomaly B in zone 2 with a surface area measuring 06 by 24 meters, anomaly C and D in zone 3 spanning approximately 115 by 125 meters and 03 by 10 meter, and anomaly D in zone 4 is measuring dimensions of roughly 140 by 120 meters, which from a geological perspective, are likely associated with exposed or concealed intrusive bodies containing magnetite rich sulfide mineralization and marked as potential drilling target zones for sulfide minerals prospection on the geological map of the Gawuch Formation of the study area (Fig. 3). This interpretation is further substantiated by our field investigations and the geological characteristics of the region. While the mineralogical and geochemical analyses by Tahirkheli et al., (2012) confirms that the hydrothermal activity tied to the ferromagnetic diorite-grandiorite rocks suggests that the igneous intrusion rather than the surrounding volcanic rocks, is the principal source of the mineralizing solutions responsible for sulfide mineralization in Kaldam Gol region. Similarly, Pudsey et al. (1985, 1985b) documented a grey diorite situated beneath the Purit Formation and faulted against the green phyllites of the Gawuch Formation, providing additional evidence that these geological features contribute to the movement and concentration of hydrothermal mineralizing fluids in the study area.

Based on the analysis of magnetic anomaly profiles, (Figs. 7b, 8b, 9b-c & 10b) the average depth to the top of anomaly sources were estimated to be approximately 7.68 meters for anomaly A, 2.47 meter for anomaly B, 16.79 meters for anomaly C, 13.61 meters for anomaly D, and 22.37 meters for anomaly E, respectively.

The interpreted 2D and 3D maps also reveals a network of structural lineaments in the study area that align with linear geological features including faults, fractures/shear zones that collectively contributes to the rugged nature of the basement topography (Hayatudeen et al., 2021). These structural elements are particularly important in mineral exploration, as many mineral deposits are located close to these fault or fracture zones (Curan et al., 1982). The dominant NE-SW orientation of the identified magnetic anomalies corresponds well with the geological strike of the surrounding host rock Gawuch Formation, indicating a strong connection between the study area's mineralization and a major NE-SW trending structural lineament, potentially a fault or fracture zone, highlighting the important role that structural features play in controlling the spatial distribution of mineral deposit in the region. The lineaments may reflect a thrusting element related to the transpressional strike-slip faulting along the Karakorum-Kohistan Suture or could be a remnant of an earlier North-South oriented compressional thrusting (Heuberger, 2004). The study area largely displays reduced magnetization, resulting in regions that appear magnetically plain or quiet zones that surround the isolated high magnetic anomalies in the area, potentially signifying an alteration zone that could be associated with underlying mineral deposits (Gunn, 1996). This interpretation is reinforced by Farhan et al. (2021a and 2021b), who identified a suite of propylitic alteration minerals such as epidote, actinolite, chlorite, albite, and pyrite with an estimated alteration temperature range of 150-300°C, indicating that the rocks in the Kaldam Gol area experienced an alteration process similar to that found in porphyry-style systems.

Supporting this prediction, the magnetic data analysis has identified a shallow and sporadic array of circular to semicircular magnetic discontinuities and alteration patterns in the study area. These geophysical characteristics are consistent with porphyry systems and imply the presence subsurface stock work of fractures and veins, which may serve as key target zones for detailed exploration and assessment of potential sulfide mineral deposits in the region.

Porphyry systems are identified by distinct geophysical attributes due to the presence of alteration halos such as propylitic, phyllic, and potassic zones, which are commonly associated with sulfide mineralization (Holden et al., 2011). In these alteration zones, magnetic susceptibility is typically enhanced in potassic alteration zones, where iron oxide minerals like magnetite are concentrated, resulting in a prominent positive or high magnetic anomaly that is often sub-circular or elliptical in shape, while magnetic susceptibility is reduced in propylitic or phyllic alteration zones, leading to a lower or negative magnetic anomaly that typically surrounds the high magnetic anomaly. (Clark et al., 1992 and 2004; Holden et al., 2011, Hope et al., 2019). This low magnetic anomaly arises from the depletion of magnetite in the volcanic host rock (Holden et al., 2010).

As noted by Clarke (2014) and Pisiak et al. (2017), magnetite serves as a significant indicator mineral for locating concealed porphyry deposits due to its prominent association with these systems, making magnetic anomalies a prevalent geophysical signature in porphyry prospecting. In the context of this study, the identified magnetic zones exhibit a distinct anomaly pattern typical of porphyry deposits. This pattern features a high magnetic core surrounded by a non-magnetic rim, a configuration that corresponds to the alteration halos commonly associated with porphyry systems. Specifically, within the study area, the central high magnetic core is likely associated with the potassic alteration zone, which is characterized by the presence of iron oxide minerals such as magnetite along with associated sulfide mineralization. Conversely, the peripheral non-magnetic minerals are interpreted as corresponding to the propylitic alteration zone, delineating the outer boundary of the mineralized region. So a thorough evaluation of the magnetic data indicates that the sulfide ore minerals present in the Gawuch Formation of Kaldam Gol regions displays key characteristics of a porphyry style mineralization which is associated with diorite-granodiorite intrusions and is structurally influenced by a NE-SW trending fault or fracture system. To further validate and refine this interpretation, it has been recommended to drill vertical and inclined exploratory core holes, targeting the high magnetic anomalous zones, to depths ranging up to 100 meters.

9. Conclusion

In the present study ground magnetic method of geophysical exploration has been employed to map the lateral heterogeneities in the Earth's magnetic field, aiming to delineate the distribution of magnetically susceptible sulfide mineralization, as well as to qualitatively map geologic structures like faults or fractures that influence the distribution of mineralization. The magnetic method has yielded detailed insights into the subsurface geological features and has successfully pinpointed and delineated numerous occurrences of sulfide minerals at relatively shallow depths within the study area.

The magnetic data analysis also reveals that the study area has been significantly influenced by dominant NE-SW structural lineaments which are responsible for hydrothermal mobilization and play a key role in controlling the spatial distribution of sulfide mineralization, which is linked to diorite-granodiorite intrusions and exhibits distinct attributes typical of porphyry-style mineralization. The quantitative analysis using Peter’s half slope and Maximum slope technique indicates that the magnetic anomaly sources in the study area range from near-surface to around 22.37 meters deep, suggesting shallow mineralization targets.

Consequently, it is concluded that the magnetic method is highly effective for delineating subsurface structural features related to sulfide mineralization, even in complex topographic and geological environments.

Acknowledgements

The authors express gratitude to the National Centre of Excellence in Geology, University of Peshawar, Pakistan for providing logistic and financial assistance for this study.

Conflicts of Interest: The authors declare no conflicts of interest.

REFERENCES

Abdulbariu, I., Ayoola, A.H., and Bala, A.J. 2016. Arewa J.O., & Fahad, A. 2024. Solid mineral potential evaluation using integrated aeromagnetic and aeroradiometric datasets. *Scientific Reports*, 14:1637.

Adegoke, J.A., and Layade, G.O., 2014. Variation of Structural Index of Peters Half Slope in Determining Magnetic Source Depth. *Archives of Physics Research*, **5(**2), 23-31.

Ademila, O., Okpoli, C.C., and Ehinmitan. D. 2019. Geological & Lithological Mapping of Part of Igarra Schist Belt Using Integrated Geophysical Methods. *Earth Sciences Pakistan*, **3**(1), 01-09.

Ajala, S.A., Salako K. A., Rafiu A. A., Alahassan U. D., Adewumi T., Sanusi Y.A. 2021. Estimation of Sedimentary Thickness for Hydrocarbon Potential over Part of Adamawa Trough, NE Nigeria Using Magnetic Method. *Earth Sciences Pakistan (ESP)*, **5**(1) ,01-05

Ali L., Moon C.J., Williamson B.J., Shah M.T., Khattak S.A., 2014b. A GIS-based stream sediment geochemical model for gold and base metal exploration in remote areas of northern Pakistan. *Arabian Journal of Geosciences* ,**8,** 5081-5093.

Ali, A., Rehman, K., Tayyeb, o., Zaman, T., Jameel, M., Khan, A., Ahmad, R., and Irfan. M. 2020. Exploring Placer Gold Deposits through integrated Geophysical & Geochemical Techniques at the confluence of the Indus & Kabul River, NW Paksitan, *Acta Geologica Sinica (English Edition)*, **94**(50): 1440-1450.

Amigun, J. O., and Adelusi, A. O. 2013. Ground Magnetic Mapping of Subsurface Structures Beneath Obanla, Federal University of Technology, Akure Nigeria: Implication for Hydrogeological Study. *Journal of Research in Sciences*, **(2):** 225-234.

Bard, J.P., Maluski, H., Matte, P.H., and Proust, F. 1980. The Kohistan sequence; Crust and mantle of an obducted island arc. *Geological Bulletin University of Peshawar*, **13**, 87-94.

Bard, J.P., 1983. Metamorphism of an Obducted Island-Arc Example of the Kohistan Sequence (Pakistan) in the Himalayan Collided Range. *Earth and Planetary*

Bignold, S., Treloar, P., 2003. Northward subduction of the Indian Plate beneath the Kohistan island arc, Pakistan Himalaya: new evidence from isotopic data. *J. Geol. Soc*. **160** (3), 377–384 *Science Letters*, **65**, 133-144.

Bignold, S.M., Treloar, P.J., Petford, N., 2006. Changing sources of magma generation beneath intra-oceanic island arcs: an insight from the juvenile Kohistan island arc, Pakistan Himalaya. Chem. Geol. 233(1–2), 46–74.

Blakely, R.J. 1996. Potential theory in Gravity and Magnetic Application, Cambridge University Press. Geomagnetic Signature and Depth Estimate of Basement Rock around Iseyin Area (Ado- Awaiye), Ibadan Southwestern Nigeria. *Journal of Geography Environment and Earth Science International*, **4**(2), 1-12

Bohai, Y.M., Mariyanto., Utama, W. 2021. Application of upward continuation filter for geomagnetic data interpretation in Gondang, Bojonegoro Area. *Journal of Marine-Rarth Science Technology*, **1**(1).

Brett, A., & Gunn, D. 2000. Applications of the vertical derivative to magnetic data interpretation. *Journal of Applied Geophysics*, **43**(3): 225-239.

Calkins, J.A., Jamiluddin, S., Kamaluddin, B., and Hussain, A. 1981. Geology and mineral resources of the Chitral-Partsan area, Hindu Kush Range, Northern Pakistan. U.S *Geological Survey Professional Paper*, 716, 33.

Chang Z., Hedenquist J.W., White N.C., Cooke D.R., Roach M., Deyell C.L., Garcia J., Gemmell J.B., McKnight S., Cuison A., 2011. Exploration Tools for Linked Porphyry and Epithermal Deposits: Example from the Mankayan IntrusionCentered Cu-Au District, Luzon, Philippines. *Economic Geology* ,**106**, 1365-1398.

Clark, D.A., 2014. Magnetic effects of Ewing. T.A., Muntener. O. 2018. The mantle source of island arc magmatism during early subduction: Evidence from Hf isotopes in rutile from the Jijal Complex, Kohistan arc, Pakistan, *Lithos*, 308-309, 262-277.

Faisal, S., Larson, K.P., Cottle, J.M., and Lamming, J. 2014. Building the Hindu Kush: monazite records of terrane accretion, plutonism and the evolution of the Himalaya–Karakoram–Tibet orogen. *Terra Nova*, **26**, 395-401.

Farhan, M., Arif, M., Ye, Y., Li, C.F., Chen, X., Schonberg, D.G., Wu, T., Ullah, Z., Hussain, Z., Zafar, T., Sadiq, I., Bukhari, S.W.H., and Khan, A. 2023**.** Fluid source and physicochemical conditions of the polymetallic mineralization in Gawuch Formation Kohistan Island Arc, NW Pakistan. *Geochemistry*, **83**.

hydrothermal alteration in porphyry copper and iron oxide copper-gold systems: a review. *Tectonophysics*, **624**, 46-65.

Clark, D.A., French, D.H, Lackie., M.A., and Schmidt, P.W. 1992. Magnetic petrology: Application of integrated rock magnetic and petrological techniques to geological interpretation of magnetic surveys. *Exploration Geophysics*, **23**, 65-68.

Cloos M. and Sapiie B. 2013. Porphyry copper deposits: strike– slip faulting and throttling cupolas. *International Geology Review* ,**55**, 43-65.

Cooper, G.R.J.; Cowan, D.R. 2006. Enhancing potential field data using filters based on the local phase. *Comput. Geosci*ences, **32**, 1585-1591.

Coward, M.P., Rex, D.C., Khan, M.A., Windley, B.F., Broughton, R.D., Luff, I.W., Petterson, M.G., Pudsey, C.J. 1986. Collision tectonics in the NW Himalayas. *Geol. Soc. Lond. Spec. Publ*. **19** (1), 203–219.

Curan, S.C., Woodruff, C.M., Thompson, E.J. 1982. Lineament analysis and inference on geologic structures – examples, from the Balcons/Ouchita trend of Texas. Geological Circular, 82-1, Bureau of Economic Geology, University of Texas at Austin,

Dobri, M.B., and Savit, C.H. 1988. Introduction to Geophysical Prospecting, 4th edn. McGraw Hill Book Co., 867.

El-Awady, M.M., El-Badrawy, H.T., El-Ela, A.M.A., Solimaan, M.R., Alrefaee, H.A., Elbowab, M. 2016. Integrated geophysical studies on the area east of Abu Gharadig basin, southern Cairo, Egypt, using potential field data. *NRIAG Journal of Astronomy and Geophysics*, xxx, xxx–xxx.

Eugene, R.P., Eveth N.A.N., Ibrahimu, K. 2019. Ground Water Potential Zones Investigation Using Ground Magnetic Survey in South Africa. Proceedings of the International Conference on Industrial Engineering and Operations Management Pretoria/ Johannesburg, South Africa, 1155-1164.

Farhan, M., Arif, M., Ying, Y., Chen, X., Garbe-Schonberg, D., Li, C.-F., Hussain, Z., Ullah, Z., Zhang, P., Khan, A. 2021a. Fluid source, element mobility and physicochemical conditions of porphyry-style hydrothermal alteration mineralization at Mirkhani, southern Chitral, Pakistan. *Ore Geol. Rev.* **135,** 1–32, 104222.

Farhan, M., Arif, M., Ying, Y., Chen, X., Garbe-Schonberg, ¨D., Ullah, Z., Sadiq, I., 2021b. Host rock peculiarities and influence of major structures on gold and base metal sulfide mineralization in northern Pakistan. *Periodico di Mineralogia*, **90** (1), 137–171.

Feyisa, H.N., and Gebissa, F.T. 2023. Geophysical Investigation of Road Failure A Case Study of Gedo-Ijaji Asphalt Road Oromia Regional State, Ethiopia. *Journal of Geology and Geophysics*,**12**(3),1-10.

Fontboté L., Kouzmanov K., Chiaradia M., Pokrovski G.S., 2017. Sulfide Minerals in Hydrothermal Deposits. *Elements*, **13**, 97-103.

Ford, K., Keating, P., and Thomas, M.D. 2007. Overview of geophysical signatures associated with Canadian ore deposits, in Goodfellow, W.D., ed., Mineral deposits of Canada. A synthesis of major deposit types, district metallogeny, the evolution of geological provinces, and exploration methods*: Geological Association of Canada, Mineral Deposits Division, Special Publication*, **5**, 939–970.

Furness, P. 2007. Modelling magnetic fields due to steel drum accumulation, *Geophys. Prospect*; **55,** 737-748

Gaboury, D., 2019. Parameters for the formation of orogenic gold deposits. Applied Earth Science, **128**, 124-133

Ganiyu, S.A., Badmus B. S., Awoyemi. M.O., Akinyemi O. D., & Olurin, O.T. 2013. Upward Continuation and Reduction to Pole Process on Aeromagnetic Data of Ibadan Area, South-Western Nigeria. *Earth Science Research***, 2(**1), 66-73.

Groves, D.I., Santosh M., Goldfarb R.J., Zhang L., 2018. Structural geometry of orogenic gold deposits: Implications for exploration of world-class and giant deposits. *Geoscience Frontiers*, **9**, 116

Gunn, P.J. 1996. Interpretation of aeromagnetic data. 1st Edn. Workshop AGSO Canberra, 1-50.

Gunn, P.J. 1997. Application of aeromagnetic surveys to sedimentary basin studies, *Journal of Australian Geology and Geophysics*, **17**(2), 105-113.

Halfpenny, R., Mazzucchelli, R.H., 1999. Regional multi-element drainage geochemistry in the Himalayan Mountains, northern Pakistan. J. *Geochem. Explor*. **67**(1–3), 223–233.

Hayatudeen, M., Rasaq, B., Onaolapo, R.I., and Olumide, A.A. 2021. First Horizontal & First Vertical Derivatives From High Resolution Aeromagnetic Data Over The Gongola Basin Upper Benue Trough Northeastern Nigeria. *Global Journal of Pure & Applied Sciences*, **27**, 181-192.

Heuberger, S. 2004. Kinematic of the Karakoram-Kohistan Suture Zone Chitral, NW Pakistan. (PhD Dissertation), Swiss Federal Institute of Technology Zurich.

Holden, J., Fu, S.C., Kovesi, P., Dentith, M., Bourne, B., Hope, M, 2011. Automatic identification of responses from porphyry intrusive systems within magnetic data using image analysis. *Journal of Applied Geophysics* ,**74,** 255–262.

Joshua, E.O., Layade, V.B., Akinboboye, V.B., Adeyemi, S.A. 2017. Magnetic mineral exploration using ground magnetic survey data of Tajimi area, Lokoja. *Global Journal of Pure & Applied Sciences*, **23**, 301-310.

Kazmi, A.H., and Jan, M.Q. 1997. Geology and Tectonics of Pakistan. Graphic Publisher, Karachi, 554.

Kearey, P., Brook, SM., and Hill, I. 2002. Introduction to geophysical exploration, 3rd edn. Blackwell Scientific Publication Oxford.

Khan, M.A., Stern, R.J., Gribble, R.F., Windley, B.F., 1997. Geochemical and isotopic constraints on subduction polarity, magma sources, and palaeogeography of the Kohistan intra-oceanic arc, northern Pakistan Himalaya. *J. Geol. Soc.* **154**(6), 935–946.

Khan, T., Khan, M.A., and Jan, M.Q. 1994. Geology of a part of the Kohistan terrain between Gilgit and Chilas, Northern Areas Pakistan. *Geological Bulletin University of Peshawar*, **27**, 99-112.

LMPL, 2022. Technical report in support of application for conversion of mineral deposit retention license (MDRL) of Laspur Mineral (Pvt) Ltd. to mining lease for Base metals, District Chitral Lower, KP, Pakistan.

Mariita, N.O. 2007. The Magnetic Method. Presented at Short Course II on Surface Exploration for Geothermal Resources, organized by UNU-GTP and KenGen, at Lake Naivasha, Kenya.

Maubana, M.W., Maryanto, S., Utami, W.I., and Nadir, A. 2019. Reservoir Magnetic Anomaly at Geothermal Area of Mount Pandan East Java Indonesia. *International Journal of Renewable Energy*, **9**, 2.

Mekonnen, T.K. 2004. Interpretation and Geodatabase of Dukes using Aeromagnetic data of Zimbabwe and Mozambique. M. Sc. Thesis, International Institute for Geo-information science and Earth Observation, Enschede, the Netherlands. Retrieved from http://www.slideserve.com/phila/partners.

Miller, H.G, Singh, V. 1994. Potential field tilt—a new concept for location of potential field sources. *J. Appl Geophys*, **32**:213–217

Milligan, P., and Gunn, P., 1997. Enhancement and presentation of airborne geophysical data. *Journal of Australian Geology & Geophysics*, **17(**2):63-75.

Mohamed, A., Abdelrady, M, Alshehri, F., Mohammed, M.A., and Abdelrady, A. 2022. Detection of Mineralization Zones Using Aeromagnetic Data. *Appl. Sci*., **12**(18),9078.

Morgan. L.A. 2012**.** Geophysical characteristics of volcanogenic massive sulfide deposits in volcanogenic massive sulfide occurrence model. U.*S Geological Survey Scientific Investigation Report*, 2010-5070-C 7,16.

Naskar, D.C., Rai, M.K. 2018. Delineation of geometry and spatial distribution of basic bodies using magnetic and resistivity methods in Sohagpur Coal Field area, Madhya Pradesh. *Journal of Research, Granthaalayah*, **6**(8):146-158.

Nettleton, L.L. 1971. Elementary Gravity and magnetic for Geologist and Seismologist Cambridge Press, 113-115.

Norman, M., Robinson, P., Clark, D., 2003. Major- and traceelement analysis of sulfide ores by laser-ablation ICP–MS, solution ICP–MS, and XRF: new data on international reference materials. *The Canadian Mineralogist*, **41**, 293-305

Nunez, D.P., Bonilla, A., Sánchez, B.L., & Prezzi, C. 2023. Potential-field filters for gravity and magnetic interpretation: A review. *Surv. Geophys*. **44**, 603–664.

Nwosu, O.B., Onuba, L.N. 2013. Evaluation of The Magnetic Basement Depth Over Parts Of Middle Benue Trough Nigeria By Empirical Depth Rule Based On Slope Techniques Using The HRAM. *International Journal of Scientific & Technology Research*, **2**(11):19-29.

Obiora, D., Idike, J., Oha, A., Chijioke, G., Ononiwu, S., Okwesili, N & Ossai, N. 2018. Investigation of magnetic anomalies of Abakaliki area, Southeastern Nigeria, using high resolution aeromagnetic data. *Journal of Geology & Mining Research*, **10**(6), 57-71.

Ogagarue, D.O., Emudianughe, J.E. 2016. Ground Magnetic Survey of the Charnokitic Dykes in the Areas Around Omu-Ijelu, Southwestern Nigeria. *IOSR Journal of Applied Physics*, **8**(3), 90-98.

Okwesili, N.A., Chiebonam, K.E., and Awucha, I.E. 2019. Euler Deconvolution and Source Parameter Imaging of aeromagnetic data of Guzabure and Gudumbali regions, Chad Basin, North Eastern Nigeria. *IOSR Journal of Applied Physics (IOSR-JAP)*, **11**(3), 01-10.

Oni, G.A., Eniola, P.J., Olorunfemi, M.O., Okunubi, M.O., Osotuyi, G.A. 2020. The magnetic method as a tool in groundwater investigation in a basement complex terrain: Modomo Southwest Nigeria as a case study, *Applied Water Science*, 10:190

Oruc, B. 2010**.** Edge Detection and Depth Estimation Using a Tilt Angle Map from Gravity Gradient Data of the Kozakli Central Anatolia Region Turkey. *Pure and Applied Geophysics*, **168**(10):1-12.

Ozegin, K.O., and Alile, O.M. 2016. Exploit of Ground Magnetic Survey Data for Solid Mineral Exploration. *International Journal of Earth Sciences Knowledge and Applications*, **3**(3):208-216.

Petterson, M.G., 2010. A Review of the geology and tectonics of the Kohistan island arc, north Pakistan. *Geological Society, London, Special Publications*, **338**, 287-327.

Petterson, M.G., and Windley, B.F. 1986. Petrological and Geochemical evolution of the Kohistan arc-batholith Gilgit, North Pakistan. *Geological Bulletin University of Peshawar*, **19**, 121-149.

Phillips, J.D. 2002. Processing and Interpretation of Aeromagnetic Data for the Santa Cruz Basin-Patahonia Mountains Area, South-Central Arizona; U.S. Geological Survey Open-File Report 02-98; U.S. Geological Survey: Reston, VA, USA.

Pisiak, L.K., Canil, D., Lacourse. T., Plouffe, A., and Ferby, T. 2017. Magnetite as an Indicator Mineral in the Exploration of Porphyry Deposits: A Case Study in Till near the Mount Polley Cu-Au Deposit British Columbia, Canada, *Economic Geology*, **112**(4), 919-940.

PMDC., 2001. Final report geochemical exploration and evaluation of gold and base metals, northern areas, Pakistan, by Pakistan Mineral Development Corporation, Islamabad

Preeti, M. 2021. Interpretation of Magnetic Data Of Cuddapah Basin India. *International Journal of Multidisciplinary Research*, **7**(10):336-341.

Pudsey, C.J., and Maguire, P.K.H. 1986. Magnetic profiles across the northern suture Kohistan, NW Pakistan. *Geological Bulletin University of Peshawar*, **19**:47-60.

Pudsey, C.J., Coward, M.P., Luff, I.W., Shackleton, R.M., Windley, B.F., and Jan, M.Q. 1985. Collision zone between the Kohistan arc and the Asian plate in NW Pakistan. *Earth and Environmental Science Transactions of the Royal Society of Edinburgh*, **76**, 463–479.

Pudsey, C.J., Schroeder, R., Skeleton, P.W., and Gupta, V.J. 1985b. Cretaceous (Aptian/Albian) age for Island arc volcanics, Kohistan, N. Paksitan, in Gupta, V.J., ed., Geology of Western Himalayas (Contributions to Himalaya Geology), Hindustan Publishing Corporation, Delhi, India, 3, 150-168.

Rasheed, A., Khattak, S.A., Ali, L., Zaib, M., Jehan, S., and Ayub, M. 2019. Geochemical profile and source identification of surface and groundwater pollution of District Chitral, Northern Pakistan. *Microchemical Journal*, **145**, 1058-1065.

Reeves, C. 2005. Aeromagnetic surveys principle practice and interpretation. Geosoft E-Publication.

Rehman, K., Ali, A., Ahmed, S., Ali, W., Ali, A., and Khan, M.Y. 2015. Spatio-temporal variations of b-value in and around north Pakistan. *Journal of Earth System Science*, **124**, 1445-1456.

Riddihough, R.P. 1971. Diurnal Corrections to Magnetic Surveys. An Assessment of Errors. *Geophysical Prospecting*, **19**, 551-567.

Saada, S.A. Edge detection and depth estimation of Galala El Bahariya Plateau, Eastern Desert-Egypt, from aeromagnetic data. *Geomech. Geophys. Geo-energ. Geo-resour.* (2015) 2:25–41.

Salati, E., Shahri, M.R.H., Karimpur, M., and Moradi, M. 2008. Ground Magnetic Survey For Exploration Of Massive Sulfide In Northeast Iran. *Journal of Applied Sciences*, **8**(22), 4051-4060.

Salem,A., Ravat, D., Gamey, T.J.. and Ushijima. K. (2002). Analytic signal approach and its applicability in environmental magnetic investigations, *J. Appl. Geophys.*, **49**, 231-244.

Schaltegger, U., Zeilinger, G., Frank, M., and Burg, J.P. 2002. Multiple mantle sources during island arc magmatism: U-Pb and Hf isotopic evidence from the Kohistan arc complex, Pakistan. *Terra Nova*, **14**, 461- 468.

Searle, M., Khan, M.A., Fraser, J., Gough, S., Jan, M.Q., 1999. The tectonic evolution of the Kohistan-Karakoram collision belt along the Karakoram Highway transect, north Pakistan. *Tectonics*, **18** (6):929–949.

Shah, M.T., and Shervais, J.W. 1999. The Dir-Utror metavolcanic sequence Kohistan arc terrane, northern Pakistan. *Journal of Asian Earth Sciences*, **17**(4):459-476.

Shahverdi, M; Namaki, L; Montahaei, M; Mesnhai, F. (2017). Interpretaion of magnetic data based on tilt derivative methods and enhancement of total horizontal gradient, a case study: Zanjan Depression. *Journal of the Earth and Space Physics*, **43**(1); 101-113.

Shehu, A. T., Nwankwo, L. I. and Salako, K. A. 2017 The Source Parameter Imaging (SPI) method for estimation of depth to buried magnetic sources from gridded digital data of the Sokoto Basin, Nigeria: Implications in exploration Geophysics. Zimbabwe. *Journal of Science & Technology*, **12**, 66–74.

Sinclair W.D., 2007. Porphyry Deposits. In: Goodfellow, W.D., Ed., Mineral Deposits of Canada: A Synthesis of Major Deposit-Types, District Metallogeny, the Evolution of Geological Provinces, and Exploration Methods, Geological Association of Canada, Mineral Deposits Division, Special Publication, Canada, Newfoundland, 223-243.

Smith, J., Brown, A. 2023. Magnetic anomaly data correction using Reduction to Pole transformation. *Geophysical Research Letters*, **45**(8), 1234-1245.

Stanely, R; Yasala S; Murugesan, R.M. 2021. Hydrological subsurface investigation using geophysical electrical and magnetic methods in and around valliyar river basin, India. *Result in Geophysical Sciences*, **7**, 100022.

Sweatman, T., Clavarino, J., Dawney, R. 1995. Drainage geochemical exploration and mineral potential of Northern Pakistan. Third report by Rex Sweatman and Associates for Australian Agency for International Development.

Tahirkheli, R.A.K., and Jan, M.Q. 1979. A preliminary geological map of Kohistan and the adjoining areas, North Pakistan. *Geological Bulletin University of Peshawar*, **11** (in pockets).

Tahirkheli, T., Khan, M.A., and Shah, M.T. 2005. Geochemistry and petrogenesis of metavolcanic rocks in Gawuch and Drosh formations Chitral, northern Pakistan. *Geological Bulletin University of Peshawar*, **38**, 189-202.

Tahirkheli, T., Shah, M.T., Khan, M.A., 1997. Lead isotopic signature of the hydrothermal copper mineralization in Droshi-Shishi Area, Chitral, Kohistan Arc Terrane, Northern Pakistan. *Geol.Bull.Univ.Peshawar*, **30,** 209–217.

Tahirkheli, T., Shah, M.T., Khan, M.A., Bilqees, R. 2012. Mineralogy and geochemistry of diorites and associated hydrothermal sulfide mineralization of Gawuch Formation in Drosh area, Chitral, northern Pakistan. *Journal of Himalayan Earth Science*, **45**(1), 31-52.

Taufiq, S., Okeke, F.N and Daniel, O.N. 2020. Interpretation of aeromagnetic data over some parts of Sokoto Basin, Nigeria, using source parameter imaging and 3D Euler deconvolution methods. *International Journal of Physical Sciences*, **15**(2), 90-98

Tawey, M.D., Alhassan, D.U., Adetona, A.A., Salako, K.A., Rafiu, A.A., and Udensi, E.E. 2020. Application of Aeromagnetic Data to Assess the Structures and Solid Mineral Potentials in Part of North Central Nigeria. *Journal of Geography Environment and Earth Science International*, **24**(5), 11-29.

Telford, W.M, Geldart, L.P AND Sherriff, R.E (2001). Applied Geophysics, 3rd edition, Cambridge University press, 632-636.

Telford, W.M., Geldart, L.P., and Sheriff, R.E. 1990. Applied geophysics, 2nd edn, Cambridge University Press, 113-114.

Thomas, M.D., Walker, J.A., Keating, P., Shives, R., Kiss, F., and Goodfellow, W.D. 2000. Geophysical atlas of massive sulfide signatures, Bathurst mining camp, New Brunswick. *Geological Survey of Canada Open File*, 3887, 105.

Thurston J.B., Smith R.S 1997. Automatic conversion of magnetic data to depth, dip, and susceptibility contrast using the SPITM method. *Geophysics*, **62**(3):807-813.

Ullah, Z., Khan, A., Faisal, S., Zafar, T., Li, H., Farhan, M., 2022a. Petrogenesis of peridotites in the Dargai Complex ophiolite, Indus Suture Zone, Northern Pakistan: implications for two stages of melting, depletion, and enrichment of the Neo-Tethyan mantle. *Lithos*, 426, 106798.

Ullah, Z., Li, H., Khan, A., Faisal, S., Dilek, Y., Forster, M.W., Farhan, M., Ashraf, U., Khattak, S.A., Rehman, G., 2022b. Mineralogy and PGE geochemistry of chromitites and peridotites of the sapat complex in the indus suture zone, northern Pakistan: implications for magmatic processes in the supra-subduction zone. *Int. Geol. Rev.* 1–26.

Verduzco B., Fairhead, J.D, Green, C.M., MacKenzie, C. 2004. New insights into magnetic derivatives for structural mapping. *Lead Edge*, **23**,116–119

Wang Y., Mao J., Chen W., Yang J., Wang Z., Yang F., 2005. Strike-slip fault controls on mineralization in the Kanggurtag gold belt in the Eastern Tianshan, Xinjiang, NW China Mineral Deposit Research: Meeting the Global Challenge. Springer, pp. 1347-1349.

Waswa, A.K., Nyamai, C.M., Mathu, E., and Ichang, D.W. 2015. Application of Magnetic Survey in the Investigation of Iron Ore Deposits and Shear Zone Delineation: Case Study of Mutomo-Ikutha Area S.E Kenya. *International Journal of Geosciences*, **6**, 729-740.

Weymouth, J.W. 1985. Geophysical surveying of archaeological sites surveying. *Archaeological Geology*. Yale University press, New Haven London, 191-235.

Zanchi, A., Gaetani, M. 2011. The geology of the Karakoram range, Pakistan: the new 1:100,000 geological map of Central-Western Karakoram. *Ital. J. Geosci*. **130**(2), 161–262.

Zeitler, P.K., 1985. Cooling history of the NW Himalaya. Pakistan. *Tectonics*, **4**(1), 127–151.